10

Theoretical study of light diffraction on multiplexed chirped multilayer diffraction structures formed in PPM-LC and PDLC

© S.N. Sharangovic, V.O. Dolgirev, D.S. Rastrygin

Tomsk State University of Control Systems and Radioelectronics, Tomsk, Russia

e-mail: daniil.rastrygin@tusur.ru

Received July 14, 2025
Revised September 02, 2025
Accepted September 12, 2025

Analytical models of light diffraction by multiplexed chirped multilayer inhomogeneous holographic diffractive structures formed in photopolymer composite materials containing nematic liquid crystals, as well as in polymer dispersed liquid crystal materials, are presented. Particular attention is paid to structures with smooth optical inhomogeneity in holographic gratings, including photopolymer materials with liquid crystals, as well as structures formed exclusively in dispersed liquid crystals..

Keywords: photopolymer materials, liquid crystals, multilayer diffraction structures, chirped, multiplexed.

DOI: 10.61011/EOS.2025.10.62567.8390-25

Introduction

Photopolymer compositions are currently regarded as one of the most promising materials for forming photonic structures [1–15]. Their primary advantages include high diffraction efficiency (DE) and technological flexibility, which enable the creation of holographic diffraction structures (HDS) with diverse geometries and parameters. Moreover, such compositions can be modified by incorporating functional additives, including liquid crystals (LCs) [5–10,15]. The addition of LCs to photopolymerizable materials unlocks further possibilities, such as controlling the DE of HDS using an external electric field. Additionally, the presence of LCs can induce unique effects, including shifts in angular selectivity, as demonstrated in several studies [8,9,15]. These properties make photopolymerizable compositions doped with LCs particularly appealing for developing adaptive optical systems and devices with tunable characteristics.

In recent years, alongside the study of single HDS, multilayer inhomogeneous holographic diffraction structures (MIHDS) have garnered increasing attention from the scientific community [16–20]. These systems hold substantial applied potential, particularly in spectral filtering tasks and the generation of ultrashort laser pulse trains. The distinctive features of MIHDS stem from their pronounced spectral-angular selectivity, whose parameters can be finely tuned by selecting the structure's architecture and materials. In particular, the angular selectivity of such structures may manifest as multiple local maxima, with its profile mirroring the selectivity characteristics of the first layer in the multilayer structure [16,20]. This indicates the potential for targeted control of the system's spectral response through variation of geometric parameters, such as the thicknesses of buffer and diffraction layers.

Thus, developing methods for effectively controlling the diffraction properties of MIHDS represents a key scientific and practical challenge. Addressing this challenge opens new avenues for creating adaptive optical systems with tunable characteristics, which could find applications in modern light processing technologies, spectroscopy, and laser physics.

One promising approach to this challenge involves using photopolymerizable compositions containing nematic liquid crystals as photosensitive media for forming MIHDS. In several studies based on MIHDS with diffraction layers made from polymer dispersed liquid crystal (PDLC) [19], it was shown that external influences not only enable regulation of diffraction efficiency but also give rise to selective characteristics in the structure. For instance, applying a voltage that suppresses diffraction of extraordinary waves in the second layer of a three-layer HDS transforms the angular selectivity of the beam diffracted in the first order, imparting properties akin to those of a two-layer HDS with an increased buffer layer density. This phenomenon arises from changes in the number of local maxima in the selective spectral response. From the perspective of optical filtering, this effect can be interpreted as alterations in the number and width of spectral channels, thereby opening new possibilities for managing the system's spectral characteristics.

In turn, the study in [21] demonstrated that external field effects on a diffraction layer formed in a photopolymer material with liquid crystals (PPM-LC) enable not only regulation of diffraction efficiency but also angular selectivity.

However, the work in [19] analyzed only a specific case involving diffraction layers based on optically homogeneous PDLC. This meant that under an external electric field, the LC director orientation changed synchronously throughout the HDS volume. At the same time, if the LC volume fraction in the composition exceeds 90% [8,15], the situation becomes more complex. In such conditions, the LC director orientation is primarily governed by the sample boundaries,

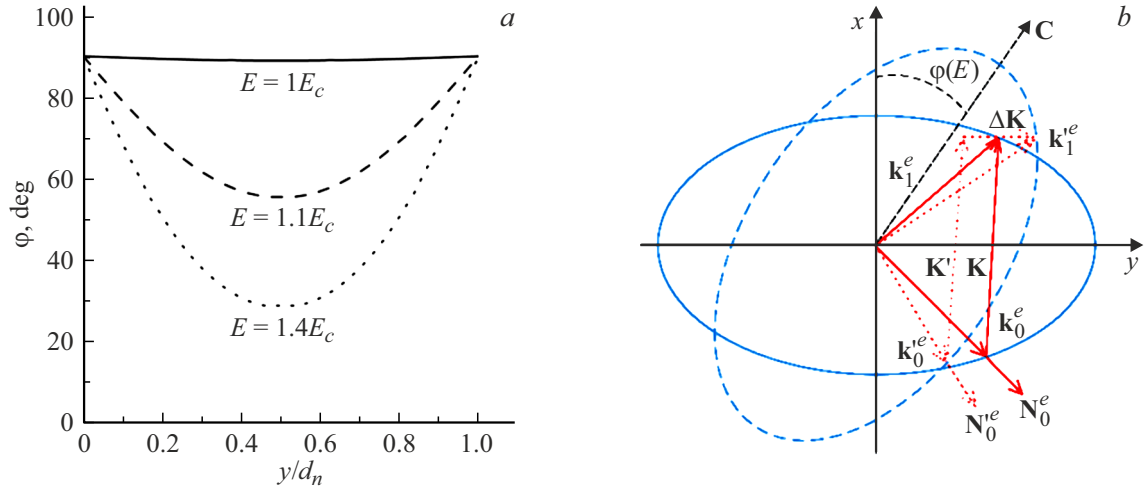

Figure 1. Dependence of the LC director rotation angle on the applied external electric field along the depth of the PPM-LC layer (*a*) and vector diffraction diagram for light *b*).

leading to optical inhomogeneity in the system. This inhomogeneity significantly affects the structure's diffraction properties and must be accounted for in modeling and analyzing light diffraction.

For multiplexed MIHDS, in which multiple diffraction layers are sequentially formed at various recording angles, substantial broadening of both angular and spectral selectivity ranges has been observed [22]. Moreover, during the creation of chirped structures, the angular selectivity width increases severalfold compared to conventional HDS [23].

The aim of this study is to continue the series of works [10–14] and present diffraction characteristics for arbitrary propagation of light beams through multiplexed chirped multilayer inhomogeneous holographic diffraction structures formed using PPM-LC- and PDLC-based materials, which exhibit smooth optical inhomogeneity along the layer direction.

Theoretical Model of Light Diffraction on MIHDS Based on PPM-LC

In describing the diffraction of plane monochromatic light waves on MIHDS, the following conditions are assumed: the aperture of the readout beam greatly exceeds the thickness of each diffraction PPM-LC layer, the recording process on the diffraction structures is fully completed, and the investigated light diffraction processes occur in the already formed structures.

At high LC contents (over 90%) in the photopolymer matrix, the LC director orientation varies throughout the depth of the diffraction layer and is determined by the sample boundaries. The director rotation angle is obtained by solving the Frederiks equation [8,15]:

$$\frac{1}{\xi_E(E)}\left(\frac{d_n}{2}+y\right)=\int_0^{\varphi(r,E)}\left(\sin^2\varphi_m(\mathbf{r},E)-\sin^2\varphi\right)^{-1/2}d\varphi, \tag{1}$$

where $\varphi_m(\mathbf{r},E)$ and $\varphi(\mathbf{r},E)$ characterize the maximum LC director rotation angle relative to the y axis along the layer depth with HDS, $\xi_E(E)=\frac{1}{E}\sqrt{\frac{4\pi K_{33}}{\Delta\varepsilon^n}}$ — the electric coherence length, K_{33} — the LC elastic coefficient, d_n — the diffraction layer thickness, n — the layer number, $\Delta\varepsilon^n=\varepsilon_{LC}^{o,n}-\varepsilon_{LC}^{e,n}\,\varepsilon_{LD}^{e,n}$, and $\varepsilon_{LC}^{o,n}$ are elements of the dielectric permeability tensor of the PPM-LC layer, measured for longitudinal and transverse director LC orientations.

When an external electric field is applied to the PPM–LC layer, director rotation begins upon exceeding the critical field strength known as the Frederiks threshold, given by:

$$E_c=\frac{\pi}{d_n}\sqrt{\frac{4\pi K_{33}}{\Delta\varepsilon}}. \tag{2}$$

Numerical solution of equation (1) for the applied electric field magnitude enabled computation of the LC director rotation angle distribution along the layer depth, as shown in Fig. 1, *a*. Fig. 1, *b* additionally presents a vector diagram illustrating light diffraction on extraordinary waves under varying LC director orientation.

Analysis of Fig. 1, *a* reveals that the LC director rotation angle varies along the diffraction layer depth and depends on the applied external electric field magnitude. In turn, changes in LC director orientation affect extraordinary wave propagation, as visually depicted in Fig. 1, *b*. The combination of these effects results in smooth optical inhomogeneity within the medium under consideration.

Consider the description of the dielectric permeability tensor for the PPM-LC material in the n-th layer of the MIHDS. Its values arise from both the LC volume fraction

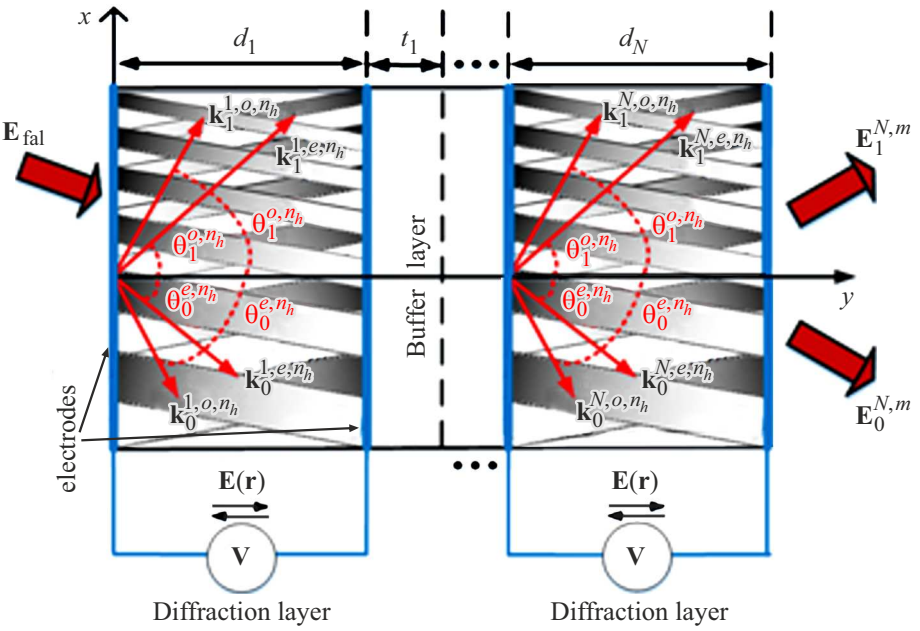

Figure 2. Schematic of light diffraction on a multiplexed chirped MIHDS with PPM-LC.

and changes in the properties of the polymer and liquid crystalline components [8]:

$$\hat{\varepsilon}^n = (1-\rho)\left(\varepsilon_p^n \hat{I} + \Delta\hat{\varepsilon}_p^n\right) + \rho\left(\hat{\varepsilon}_{LC}^n + \Delta\hat{\varepsilon}_{LC}^n\right), \qquad (3)$$

Here, ρ — the LC volume fraction in the n-th layer, $\hat{\mathbf{I}}$ — the unit tensor of the respective layer, $\varepsilon_p^n = (n_p)^2$ — the dielectric permeability of the polymer matrix, $\hat{\varepsilon}_{LC}^n$ — the LC dielectric permeability tensor, which depends on the LC director orientation and is given by:

$$\hat{\varepsilon}_{LC}^n = \varepsilon_0^n \hat{\mathbf{I}} + \Delta\varepsilon^n \mathrm{CC}, \qquad (4)$$

where C — the LC director, $n = 0 \ldots N$, N — the number of layers.

Changes in the dielectric permeability tensor are expressed via Fourier series expansion over the lattice spatial harmonics. Taking into account that $\Delta\hat{\varepsilon}_p^n\delta \ll \varepsilon_p^n$ and $\Delta\hat{\varepsilon}_{LC}^n\delta \ll \hat{\varepsilon}_{LC}^n$

$$\Delta\hat{\varepsilon}_p^n \Delta\varepsilon_{0,p}^n + \sum_{j=1}^{N} \Delta\hat{\varepsilon}_{j,p}^n \cos(j\mathbf{Kr}),$$

$$\Delta\hat{\varepsilon}_{LC}^n = \Delta\hat{\varepsilon}_{0,LC}^n + \sum_{j=1}^{N} \Delta\hat{\varepsilon}_{j,JC}^n \cos(j\mathbf{Kr}),$$

where $\mathbf{r}$ — the position vector, $\mathbf{K}$ — the grating vector, and $\Delta\varepsilon_{j,p}^n$ and $\Delta\varepsilon_{j,LC}^n$ are defined as [8,11]

$$\Delta\hat{\varepsilon}_{j,p}^n = 2n_p^n \Delta n_{j,p}^n \hat{\mathbf{I}},$$

$$\Delta\hat{\varepsilon}_{j,LC}^n = 2\left(n_o \Delta n_{j,e}^n \hat{\mathbf{I}} + (n_0 \Delta n_{j,o}^n - n_e \Delta n_{j,e}^n)\mathbf{CC}\right),$$

Consequently, expression (3) shows that the overall change in the dielectric permeability tensor is determined by the LC director orientation, which in turn depends on the applied electric voltage magnitude.

For the mathematical description of the diffraction problem, it is assumed that a quasi-monochromatic light beam with arbitrary polarization, characterized by the amplitude profile $\mathbf{E}^0$, wave vector $\mathbf{k}_0$ and unit complex polarization vector $\mathbf{e}^0$forming an angle θ_{fal} with the optical axis of the structure, impinges on the multilayer inhomogeneous holographic diffraction structure. A schematic representation of the light diffraction process on the MIHDS consisting of N layers is shown in Fig. 2.

The incident quasi-plane light wave at the interface is represented as a superposition of eigenwaves [19]:

$$\mathbf{E}^0(\mathbf{r}, t) = \frac{1}{2}\left[\sum_{m=o,e} \int_{-\infty}^{\infty} \mathbf{e}_0^m E^{0,m}(\omega, \mathbf{r}) \times \exp\left[i\left[(\omega_0 + \omega)t - \mathbf{k}_0^m \cdot \mathbf{r}\right]\right] d\omega + \mathrm{c.c}\right],$$

here ω_0 — central frequency, $\mathbf{e}_0^m$ — unit polarization vector, $\mathbf{k}_j^m = kn_j^m \mathbf{N}_j^m$, $k = 2\pi/\lambda$, λ — wavelength, $\mathbf{N}_j^m$ — wave normal, index $m$taking values o and $e$corresponds to ordinary and extraordinary waves respectively, n_j^m — refractive index of the HDS.

Accounting for the optical inhomogeneity of the PPM-LC-based medium, the propagation of the light field in the interaction region is described within the two-dimensional Bragg diffraction approximation using the slowly varying

amplitude (SVA) method [14]:

$$\mathbf{E}(\mathbf{r},t)=\frac{1}{2}\left[\sum_{m}^{o,e}\sum_{j}^{0,1}\int_{-\infty}^{\infty}\mathbf{e}_j^m E_j^m(\omega,\mathbf{r})\right.$$

$$\left.\times\exp\left[i\left((\omega_0+\omega)t-\int_0^r\mathbf{k}_j^m(\mathbf{r})\mathbf{r}d\mathbf{r}\right)\right]d\omega+\text{c.c.}\right],\quad(5)$$

Here, the amplitudes $E_j^m(\omega,\mathbf{r})$ are treated as slowly varying functions computed based on the first-order SVA equations, where $j=0,\ 1$ corresponds to diffraction orders.

The refractive indices and polarization parameters of the light waves involved in equation (5) are calculated using the zero-order SVA equations [8]:

$$\left[n_j^{n,m2}\left(\hat{\mathbf{I}}-\mathbf{N}_j^m\mathbf{N}_j^m\right)-\hat{\varepsilon}_0^n(\mathbf{r})\right]\mathbf{e}_j^m=0.$$

Under Bragg diffraction conditions for light on multilayer inhomogeneous holographic diffraction structures containing optically inhomogeneous PPM-LC layers, and in accordance with the SVA method, the amplitudes of interacting waves can be determined from the coupled wave equations (CWEs) in partial derivatives [8,15,18]:

$$\mathbf{N}_{r0}^{m,n}\nabla E_0^{m,n}(\omega,\mathbf{r})=-iC_1^{m,n}(E)n_1^{m,n}$$
$$\times(\mathbf{r},E)E_1^{m,n}(\omega,\mathbf{r})\cdot\exp\left[+i\Theta^{m,n}(\mathbf{r},E)\right],$$
$$\mathbf{N}_{r0}^{m,n}\nabla E_0^{m,n}(\omega,\mathbf{r})=-iC_1^{m,n}(E)n_1^{m,n}$$
$$\times(\mathbf{r},E)E_1^{m,n}(\omega,\mathbf{r})\cdot\exp\left[-i\Theta^{m,n}(\mathbf{r},E)\right],\quad(6)$$

here $C_j^{m,n}(E)=\omega(\mathbf{e}_1^m\Delta\varepsilon^n(\mathbf{r})\mathbf{e}_0^m)(c_c n_{1,0}^{m,n}\cos\beta_{1,0}^m)^{-1}/4$ — coupling coefficients, $n_1^{m,n}$ — normalized refractive index profile of the first HDS harmonic, $\Theta^{m,n}(\mathbf{r},E)$ — integral phase mismatch, defined as [8,15]:

$$\Theta^{m,n}(\mathbf{r},E)=\int_0^{d_n}\Delta\mathbf{K}^{m,n}(\mathbf{r},E)d\mathbf{r},\quad(7)$$

where $\Delta\mathbf{K}^{m,n}=\mathbf{k}_0^{m,n}-\mathbf{k}_1^{m,n}+\mathbf{K}^{m,n}=\Delta K^{m,n}\mathbf{p}^{m,n}$ — local phase mismatch, $\mathbf{p}^{m,n}$ — unit vector defining the direction of the local phase mismatch $\Delta\mathbf{K}^{n,m}$.

Given that the LC director rotation angle varies along the depth of the diffraction layer under the influence of an external electric field, the refractive index for extraordinary waves entering the coupling coefficients varies at each point in the sample as follows:

$$n_{1,0}^{e,n}(\mathbf{r},E)=n_0 n_e\left[n_0^2\cos^2(\varphi^n(\mathbf{r},E)\pm\theta_{1,0}^{e,n})\right.$$
$$\left.+n_0^2\cos^2(\varphi^n(\mathbf{r},E)\pm\theta_{1,0}^{e,n})\right]^{-1/2}.\quad(8)$$

The value $\varphi^n(\mathbf{r},E)$ is determined from equation (1), while n_0 and n_e correspond to the ordinary and extraordinary refractive indices of the liquid crystals.

As demonstrated in [8,15], expression (7) exhibits complex functional dependence, rendering equations (6) analytically unsolvable in general form. However, applying parabolic approximation to expression (7) enables obtaining CWE solutions for each individual layer. Consequently, for given extraordinary wave normal directions $\mathbf{N}_j^{e,n}$ the integral phase mismatch parameter $\Theta^{e,n}(\mathbf{r})$ can be represented as [8,15]:

$$\Theta_1(y_1,E)=\Theta_0+a_1(E)y_1+b_1(E)y_1^2,\quad\text{at}\ \ n=1,$$
$$\Theta_1(y_n,E)=\Theta_{n-1}+a_n(E)y_n+b_n(E)y_n^2,$$
$$\text{at}\quad n=2,\ \ldots,\ N,\quad(9)$$

where θ_0 — initial integral phase mismatch value, $a_n(E)$ and $b_n(E)$ — parabolic approximation coefficients determining the phase shift variation character along the layer depth. Parameter $y_n=0\ldots d_n$ — current coordinate within the n-th layer, satisfying the condition $Q=\lambda d_n/\Lambda^2\geq 1$ for Bragg diffraction regime.

The spatial variation of wave vectors $\mathbf{k}_j^{m,n}(\mathbf{r})$ within each layer, accounting for smooth optical inhomogeneity, can be approximated using a linear dependence represented as a Taylor series expansion [8,15]:

$$\mathbf{k}_j^{e,n}(\mathbf{r})\approx\mathbf{k}'^{e,n}_j+\left.\frac{d\mathbf{k}_s^{e,n}}{d\mathbf{r}}\right|_{r=0}=\mathbf{k}'^{e,}_j+k_j^{e,n}\mathbf{N}'^{e,n}_j$$
$$\times\left[\left.\frac{dn_j^{e,n}}{d\mathbf{r}}\right|_{\mathbf{r}=0}\mathbf{r}\right]+k_j^{e,n}n'^{e,n}_j\left[\left.\frac{d\mathbf{N}_j^{e,n}}{d\mathbf{r}}\right|_{\mathbf{r}=0}\mathbf{r}\right],\quad(10)$$

where wave vectors $\mathbf{k}'^{e,n}$, wave normals $bfN'^{\mathbf{e},\mathbf{n}}_j$ and extraordinary wave refractive index $n'^{e,n}_j$ are taken at $\mathbf{r}=0$.

Substituting the wave vectors from equation (10) into the expression for local phase mismatch $\Delta\mathbf{K}^{m,n}(\mathbf{r})$, the vector component $\Delta\mathbf{K}^{m,n}(\mathbf{r})=\Delta K_y^{m,n}\mathbf{y}_0$is determined as:

$$\Delta\mathbf{K}^{m,n}\cdot\mathbf{y}_0=\Delta K_0^{m,n}+t_y^n y,\quad(11)$$

where $\mathbf{y}_0$ — unit vector, $\Delta K_0^{m,n}$ — y-component of vector $\Delta\mathbf{K}_0^{m,n}(\mathbf{r})$taken at $\mathbf{r}=0$, and coefficient t_y^n can be expressed as [8,15]

$$t_y^n=k_0^{e,n}\left[(y_0N_0^{e,m})(y_0\nabla n_0^{e,n})-(y_0N_1^{e,n})(y_0\nabla n_1^{e,n})\right.$$
$$\left.+\frac{(y_0\mathbf{m}_0^{e,n})(\mathbf{m}_0^{e,n}\nabla n_0^{e,n})}{(N_{r0}^{e,n}y_0)}-\frac{(y_0\nabla n_1^{e,n})\mathbf{m}_1^{e,n}\nabla n_1^{e,n}}{(N_{r1}^{e,n}y_0)}\right]\quad(12)$$

where $\mathbf{m}_j^{e,n}$ — unit vector of the hodograph described by the end of wave vector $\mathbf{k}_j^{e,n}$, $\nabla n_{0,1}^{e,n}$ — refractive index variation.

Ultimately, the integral phase mismatch $\Theta^{m,n}(\mathbf{r},E)$used in CWEs (6), accounting for the vector component $\Delta\mathbf{K}^{m,n}(\mathbf{r})$ from expression (11), can be represented in analytical form as [8,15]:

$$\Theta^{m,n}(\mathbf{r},E)=\int\Delta\mathbf{K}^{m,n}(\mathbf{r})d\mathbf{r}=\int(\Delta K^{m,n}\mathbf{y}_0)d(\mathbf{y}_0y)$$
$$=\int\Delta K_y^{m,n}dy=\Delta K_0^{m,n}y+\frac{t_y^n}{2}y^2.\quad(13)$$

Comparing the integral phase mismatch expressions from formulas (9) and (13), the following relation can be derived with high accuracy:

$$\Theta_{\text{start}} = 0, \quad a_n(E) = \Delta K_0^{m,n},$$

$$b_n(E) = t_y^n/2, \quad \text{where} \quad n = 1 \ldots N.$$

Thus, interlayer interactions are determined by the integral phase mismatch elements Θ^{n-1}. To solve equations (6), it is necessary to approximate parameter $\Theta^{m,n}(\mathbf{r})$ in each layer and determine coefficients a_n and b_n from expression (9) by minimizing the integral mean square approximation error [8,15]:

$$er^n(y) = \frac{1}{d_n \sqrt{\int\limits_0^d \left(\Omega^{m,n}(y) - \Theta^{m,n}(y_n, E)\right)^2 dy_n}},$$

here $\Theta^{m,n}(y)$ — integral phase mismatch parameter from expression (6), $\Theta^{m,n}(y_n, E)$ — approximating function of the n-th layer determined by equations (9).

After deriving analytical expressions for integral phase mismatch and wave vectors along the photopolymer-liquid crystal structure layers, formulas describing the spatial amplitude distributions of light fields for zero and first diffraction orders at the output of the multilayer inhomogeneous holographic diffraction structure can be obtained [8,15]:

$$\mathbf{E}_1^n(\eta) = \mathbf{e}_1^{o,n} E_1^{o,n}(\eta) \exp\left[-i \int\limits_0^{d_n} \mathbf{k}_1^{o,n} d\mathbf{r}\right]$$

$$+ \mathbf{e}_1^{e,n} E_1^{e,n}(\eta) \exp\left[-i \int\limits_0^{d_n} \mathbf{k}_1^{e,n} d\mathbf{r}\right],$$

$$\mathbf{E}_0^n(\xi) = \mathbf{e}_0^{o,n} E_0^{o,n}(\xi) \exp\left[-i \int\limits_0^{d_n} \mathbf{k}_0^{o,n} d\mathbf{r}\right]$$

$$+ \mathbf{e}_0^{e,n} E_0^{e,n}(\eta) \exp\left[-i \int\limits_0^{d_n} \mathbf{k}_0^{e,n} d\mathbf{r}\right],$$

where $\mathbf{E}_j^{m,n}$ — polarization vectors, $\xi_0 = \xi$, $\xi_1 = \eta$, ξ_0, ξ_1 — aperture coordinates.

The transformation process of plane light waves passing through multilayer media is conveniently described using the matrix method. This requires transitioning from amplitude distributions of frequency Fourier components of diffracting beams to their corresponding angular spectra:

$$E_j^e(\theta) = \int\limits_{-\infty}^{\infty} E_j^e(l) \exp[ik_j^e l\theta] dl,$$

where $l = \xi_0,\ \xi_1$, angle θ characterizes the direction of plane wave components $E_j^e(\theta)$ relative to wave normals.

Thus, the transformation of frequency-angular spectra (FAS) of light beams on extraordinary waves passing through MIHDS with embedded PPM-LC layers reduces to sequential multiplication of transfer function matrices of all layers by the input optical field vector [8,18]:

$$\mathbf{E}^{e,n} = \mathbf{T}^{e,n} \mathbf{E}^0, \tag{14}$$

where $\mathbf{T}^N = \mathbf{T}^{e,N} \cdot \mathbf{A}^{e,N-1} \cdot \mathbf{T}^{e,N-1} \cdot \ldots \cdot \mathbf{A}^{e,n} \mathbf{T}^{e,n} \ldots \mathbf{A}^{e,1} \mathbf{T}^{e,1}$ — matrix transfer function of the entire MIHDS,

$$\mathbf{E}^{e,N} = \begin{bmatrix} E_0^{e,N}(\omega, \theta) \\ E_1^{e,N}(\omega, \theta) \end{bmatrix},$$

$$T^{e,n} = \begin{bmatrix} T_{00}^{e,n}(\omega, \theta) & T_{10}^{e,n}(\omega, \theta) \\ T_{01}^{e,n}(\omega, \theta) & T_{11}^{e,n}(\omega, \theta) \end{bmatrix}$$

— matrix transfer function,

$$\mathbf{E}^0 = \begin{bmatrix} E_0(\omega, 0) \\ 0 \end{bmatrix},$$

$\mathbf{A}^{e,n}$ — transition matrix for the buffer layer accounting for phase shift under equal refractive indices of diffraction and buffer layers. It can be expressed as [19]:

$$\mathbf{A}^{e,n} = \exp\left[-i(\mathbf{k}_1^{e,n} \mathbf{y}_0) t_n\right] \begin{bmatrix} 1 & 0 \\ 0 & \exp\left[\frac{-i\Delta K^{e,n} t_n}{d_n}\right] \end{bmatrix},$$

where t_n — buffer layer thickness.

Elements of matrix $\mathbf{T}^{e,n}$ are expressed as [8]

$$T_{00}^{e,n} = -\frac{C_0^{e,n} C_1^{e,n} d_n^2}{4\nu_1 \nu_0} \int\limits_{-1}^{+1} \exp\left[\delta m'(1-y) + \delta^2 n'(1-y)^2\right]$$

$$\times \Phi\left(\frac{d'}{b'} + 1, 2; b'\delta^2 \frac{\nu_1}{\nu_0}(1-y^2)\right) dy(1+y),$$

$$T_{10,01}^{e,n} = -i\frac{C_1^{e,n} d_n}{2\nu_0} \int\limits_{-1}^{+1} \exp\left[\delta m'(1-y) + \delta^2 n'(1-y)^2\right]$$

$$\times \Phi\left(\frac{d'}{b'}, 1; b'\delta^2 \frac{\nu_1}{\nu_0}(1-y^2)\right) dy,$$

$$T_{01}^{e,n} = -i\frac{C_1^{e,n} d_n}{2\nu_1} \int\limits_{-1}^{+1} \exp\left[\delta m'(1-y) + \delta^2 n'(1-y)^2\right]$$

$$\times \Phi\left(\frac{d'}{b'}, 1; b'\delta^2 \frac{\nu_1}{\nu_0}(1-y^2)\right) dy,$$

$$T_{11}^{e,n} = -i\frac{C_0^{e,n} C_1^{e,n} d_n^2}{4\nu_1 \nu_0} \int\limits_{-1}^{+1} \exp\left[\delta m(1-y) + \delta^2 n(1-y)^2\right]$$

$$\times \Phi\left(\frac{d'}{a} + 1, 2; a\delta^2 \frac{\nu_1}{\nu_0}(1-y^2)\right) dy(1+y),$$

$\Phi(a, b; c)$ — confluent hypergeometric function of the first kind, for $n = 1$, $T_{10}^{e,n} = 0$ and $T_{11} = 0$, $\delta = d_n(\eta_1\nu_0 - \eta_0\nu_1)/2\nu_1$, $\eta_j = \eta_j^{e,n} = \pm\sin\theta_{rj}^{e,n}$, $\nu_j = \nu_j^{e,n} = \cos\theta_{rj}^{e,n}$, $\theta_{rj}^{e,n}$ — angles between group normals $N_{rj}^{e,n}$ and the $y$axis,

$$m = \eta(-a + b\nu_1/\nu_0) - i\Delta K' d_n/2\delta,$$

$$m' = \xi(-a'/2 + b'\nu_1/\nu_0) - i\Delta K' d_n/2\delta,$$

$$n' = \frac{b'\nu_1}{\nu_0} - \frac{a'}{2}, \qquad a = i\frac{t_y^n \nu_1\nu_0}{(\eta_1\nu_0 + \eta_0\nu_1)^2},$$

$$a' = -i\frac{t_y^{n2}\nu_1}{(\eta_1\nu_0 + \eta_0\nu_1)^2}, \qquad b = i\frac{t_y^n \nu_0^2}{(\eta_1\nu_0 + \eta_0\nu_1)^2},$$

$$n = \frac{\nu_1}{\nu_0}\left(a - \frac{b\nu_1}{2\nu_0}\right), \qquad b' = -i\frac{t_y^n \nu_1\nu_0}{(\eta_1\nu_0 - \eta_0\nu_1)^2},$$

$$\sigma = \frac{C_0^{e,n} C_1^{e,n}}{(\eta_1\nu_0 - \eta_0\nu_1)^2}, \qquad d' = -\sigma^2.$$

In the special case of plane wave interaction in MIHDS based on HDS with uniform profiles, the transition matrix elements reduce to known expressions [15].

Theoretical Model of Light Diffraction on MIHDS Based on PDLC

Within the proposed mathematical model, the diffraction characteristics of light passing through multiplexed, chirped multilayer inhomogeneous holographic structures containing encapsulated polymers with liquid crystals are investigated. The diffraction scheme for PDLC fully corresponds to the scheme presented for photopolymer materials with liquid crystals shown in Fig. 2.

Additionally, the phase profile $\varphi_c^n(\mathbf{r})$ of the chirped structure for each layer will be accounted for according to the methodology described in [23]

$$\varphi_c^n(\mathbf{r}) = \varphi_0^n + \nabla\varphi^n \mathbf{r} + 0,5\nabla^2\varphi^n \mathbf{r}^2, \tag{15}$$

where $\nabla\varphi^n = \mathbf{K}_0^n$ is the average value, $0,5\nabla^2\varphi^n$ — quadratic coefficient of the grating vector magnitude Kvariation.

The developed mathematical model characterizing light diffraction on multiplexed chirped multilayer diffraction structures with EPLC relies on a system of coupled wave equations expressed through partial derivatives. This system enables computation of amplitude profiles of light beams $E_j^{n,m,h}$ interacting with each diffraction structure [24,25]:

$$\begin{cases} \mathbf{N}_{r0}^{n,m,n_h}\nabla E_0^{n,m,n_h}(\mathbf{r}) = - \\ \qquad iC_1^{n,m,n_h} E_1^{n,m,n_h}(\mathbf{r})\exp(i\Delta\mathbf{K}^{n,m,n_h}\mathbf{r}) \\ \mathbf{N}_{r1}^{n,m,n_h}\nabla E_1^{n,m,n_h}(\mathbf{r}) = - \\ \qquad iC_0^{n,m,n_h} E_0^{n,m,n_h}(\mathbf{r})\exp(i\Delta\mathbf{K}^{n,m,n_h}\mathbf{r}) \end{cases}, \tag{16}$$

In this system, group normal vectors are denoted as N_{rj}^{n,m,n_h} characterizing light wave propagation direction. Parameter E_j^{n,m,n_h} describes the spatial amplitude distribution of light beam profiles. Parameter C_j^{n,m,n_h} defines amplitude coupling coefficients. Parameter n_n^{n,m,n_h} characterizes the normalized amplitude profile of the diffraction structure refractive index, while the phase mismatch vector is specified through $\Delta K^{n,m,n_h} = K^{n,m,n_h} + \mathbf{k}_0^{n,m,n_h}\mathbf{k}_1^{n,m,n_h}$, n_h — number of the corresponding HDS.

The coupling coefficients C_j^{n,m,n_h} included in the coupled wave equation (16), as shown in [24], can be expressed as:

$$\begin{cases} C_0^{n,m,n_h} = \frac{1}{4}\frac{\omega}{c_c n_0^{n,mn_h}}\mathbf{e}_1^{n,m,n_h}\Delta\hat{\boldsymbol{\varepsilon}}_{n,n_h}\mathbf{e}_0^{n,m,n_h} \\ C_1^{n,m,n_h} = \frac{1}{4}\frac{\omega}{c_c n_1^{n,mn_h}}\mathbf{e}_0^{n,m,n_h}\Delta\hat{\boldsymbol{\varepsilon}}_{n,n_h}\mathbf{e}_1^{n,m,n_h} \end{cases}, \tag{17}$$

where $\mathbf{e}_j^{n,m,n_h}$ — unit polarization vector for each light beam, ω — angular frequency of the transmitted radiation, parameter $\Delta\hat{\boldsymbol{\varepsilon}}^{n,n_h}$ defines the amplitude of the first harmonic perturbation of the dielectric permeability tensor, n_j^{n,m,n_h} — refractive index for each light beam.

As demonstrated in the study [23], the refractive indices n_j^{n,m,n_h} and corresponding polarization vectors $\mathbf{e}_j^{n,m,n_h}$ are determined from the equation

$$\left[\left(n_j^{n,m,n_h}\right)^2\left(\hat{\mathbf{I}} - \mathbf{N}_j^{n,m,n_h}\mathbf{N}^{n,m,n_h}\right) - \Delta\hat{\boldsymbol{\varepsilon}}^{n,m,n_h}\right]\mathbf{e}_j^{n,m,n_h} = 0, \tag{18}$$

where vector $\mathbf{N}_j^{n,m,n_h}$ defines the direction of the optical beam wavefront propagation, $\Delta\hat{\boldsymbol{\varepsilon}}^{n,n_h}$ — tensor characterizing the medium's dielectric permeability in the absence of perturbations.

The phase mismatch described by expression (17) reflects deviation from ideal Bragg diffraction conditions and arises from several factors. These include changes in the frequency (or wavelength) of the incident radiation, deviation of the light beam incidence angle from the optimal value, and effects of external fields such as electric, magnetic, or mechanical, which introduce additional structural distortions. These factors significantly impact diffraction characteristics and must be accounted for in theoretical modeling and investigation of multilayer structure optical properties.

In this work, the primary focus is on analyzing the impact of external electric fields on the diffraction characteristics of the structure under consideration. Within the adopted model, phase mismatch is assumed to depend linearly on two key parameters: the incidence angle and frequency of the probe radiation, consistent with findings in [26].

An external electric field applied to the recorded holographic diffraction structure in an encapsulated polymer-liquid crystal composite medium induces reorientation of the liquid crystal droplet directors. This reorientation causes substantial transformation of the system's optical parameters, determining changes in its diffraction and polarization properties. As established in [27], the dependence of the director rotation angle in liquid crystal microcapsules on the

applied field can be described by:

$$\varphi_{\text{ext}}(\mathbf{r}, E) = \frac{1}{2}\,\text{arctg}\left[\cos(2\varphi_0)/(e^2(E) + \sin(2\varphi_0))\right], \tag{19}$$

where parameter

$$e(E) = E(\mathbf{r})R\sqrt{\Delta\bar{\varepsilon}(5,\, 7\delta^2 + 2,\, 1\lambda_\Pi)}$$

describes the electric field influence on the orientation of bipolar droplets containing liquid crystals, parameter R defines the droplet radius with LCs, δ determines the droplet eccentricity, parameter$\Delta\bar{\varepsilon}$ — effective dielectric anisotropy characteristic of bipolar droplets [27], $\lambda_\Pi = RW_a/K_{33}$ characterizes the interaction between the droplet surface and LCs, whereW_a reflects the degree of azimuthal surface anchoring, K_{33} defines the Frank elastic constant value. Angle φ_0 specifies the angle between the electric field strength vectors $\mathbf{E}$ and LC director $\mathbf{C}$ in the absence of electric field.

The refractive indices $n_j^{n,m,n_h}(\mathbf{r}E)$ entering expression (17) can be determined based on the LC capsule director rotation condition [28]:

$$n_{0,1}^{n,m,n_h}(\mathbf{r}, E) = \frac{n_{LC}^o N_{LC}}{[(n_{LC}^e)^2\sin^2(\varepsilon_{\text{ext}}^n(\mathbf{r}, E)\pm\theta_0^m)+(n_{LC}^o)^2\cos^2(\varphi_{\text{ext}}^n(\mathbf{r}, E)\pm\theta_0^m)]}. \tag{20}$$

The conducted analysis shows that variations in refractive indices in EPLC structures under applied electric field lead to substantial changes in the coupling coefficient magnitudes presented in equation (17):

$$\begin{cases} C_0^{n,m,n_h}(\mathbf{r}, E) \\ = \frac{1}{4}\frac{\omega}{c_c n_0^{n,m,n_h}(\mathbf{r},E)}\mathbf{e}_1^{n,m,n_h}(\mathbf{r}, E)\cdot\Delta\hat{\varepsilon}(E)\mathbf{e}_1^{n,m,n_h}(\mathbf{r}, E) \\ C_1^{n,m,n_h}(\mathbf{r}, E) \\ = \frac{1}{4}\frac{\omega}{c_c n_0^{n,m,n_h}(\mathbf{r},E)}(\mathbf{r}, E)\cdot\Delta\hat{\varepsilon}(E)\mathbf{e}_0^{n,m,n_h}(\mathbf{r}, E) \end{cases} \tag{21}$$

Vectors $\mathbf{e}_j^{n,m,n_h}(\mathbf{r}, E)$ used in (21) can be determined from expression (18), taking into account the conditions from (20).

Application of an external electric field induces angular orientation of liquid crystal microcapsule directors, giving rise to a phase mismatch vector. According to theoretical derivations in [26], this vector can be expressed as:

$$\Delta\mathbf{K}^{n,m,n_h}(\mathbf{r}, E) = \mathbf{K}^{n,m,n_h} + \mathbf{k}_0^{n,m,n_h}(\mathbf{r}, E) - \mathbf{k}_1^{n,m,n_h}. \tag{22}$$

The angular change in director orientation in liquid crystal microcapsules is spatially uniform throughout the sample depth. This fact indicates that the magnitude of phase distortions remains constant, independent of the diffraction structure's geometric thickness. Thus, phase mismatch variations can be described by expression (22).

Determination of director angular orientation in a liquid crystal microcapsule can be performed by solving the equation establishing director orientation as

$$\mathbf{C}^n(\mathbf{r}, E) = \begin{bmatrix} \sin(\pi/2 - \varphi_{\text{ext}}(\mathbf{r}, E)) \\ \sin(\varphi_0) \\ \cos(\pi/2 - \varphi_{\text{ext}}(\mathbf{r}, E)) \end{bmatrix}, \tag{23}$$

where φ_0 — initial director orientation angle.

The perturbed dielectric permeability tensor for PDLC layers has the form [28,29]

$$\hat{\varepsilon}^{n,n_h}(\mathbf{r}, E) = (1-\rho)\left[\varepsilon_p\hat{\mathbf{I}} + \sum_{m=0,e}\Delta\hat{\varepsilon}_p^{n,m,n_h}(\mathbf{r})\right] + \rho\left[\hat{\varepsilon}_{LC}^n + \sum_{m=0,e}\Delta\hat{\varepsilon}_{LC}^{n,m,n_h}(\mathbf{r}, E)\right], \tag{24}$$

where $\Delta\hat{\varepsilon}_p^{n,m,n_h}$ and $\Delta\hat{\varepsilon}_{LC}^{n,m,n_h}(\mathbf{r}, E)$ — changes in the dielectric permeability tensor for polymer and LC components.

The change in the dielectric permeability harmonic amplitude of the liquid crystal component is determined as

$$\Delta\hat{\varepsilon}_{LC}^{nmn_h}(\mathbf{r}, E) = 2(n_0 n_{LC}^{n,e}(\mathbf{r}) - n_e n_{LC}^{n,e}(\mathbf{r})) \times \int_0^\pi\int_{-1}^1 \mathbf{C}^n(\mathbf{r}, E)\mathbf{C}^n(\mathbf{r}, E)p(\alpha)q(\varphi)d\alpha d\varphi, \tag{25}$$

where α and φ — angles characterizing liquid crystal molecule orientation within the ellipsoidal capsule, and director direction $\mathbf{C}^n(\mathbf{r}, E)$ is described by formula (23).

Use of matrix analysis apparatus provides the theoretical basis for studying the interrelationship between zero- and first-order diffraction light fields in the n-th layer of a multilayer diffraction structure.

The resulting light field distribution at the output of multiplexed chirped MIHDS can be obtained by sequential multiplication of transmission matrices describing diffraction and buffer layers by the input optical field, as shown in [19]:

$$\mathbf{E}^{N,m} = \left(\mathbf{T}_h^{N,m,1} + \ldots T_h^{N,m,N_h} + \ldots T_h^{N,m,N_h}\right)\mathbf{E}^0, \tag{26}$$

where

$$\mathbf{E}^{n,m} = \begin{bmatrix} E_0^{N,m}(E, \Delta K) \\ E_1^{N,m}(E, \Delta K) \end{bmatrix}$$

defines the output optical field, $E_j^{N,m}(E\Delta K)$ shows the frequency-angular spectra at the output of the N-th layer of multiplexed MIHDS,

$$\mathbf{T}_h^{N,m,n_h} = \mathbf{T}^{N,m,m_h}\mathbf{A}^{N-1,m}\mathbf{T}^{N-1,m,n_h}\ldots\mathbf{A}^{1,m}\mathbf{T}^{1,m,n_h}$$

is the matrix transfer function for the entire MIHDS for the n_h hologram,

$$\mathbf{T}^{n,m,n_h} = \begin{bmatrix} \mathbf{T}_{00}^{n,m,n_h}(E, \Delta K) & \mathbf{T}_{10}^{n,m,n_h}(E, \Delta K) \\ T_{01}^{n,m,n_h}(E\Delta K) & \mathbf{T}_{11}^{n,m,n_h}(E, \Delta K) \end{bmatrix}$$

— matrix transfer function for the n-th layer and n_h hologram with matrix function elements $T_h^{N,m,n_h}[0, 0]$ characterizing light field coupling between different diffraction PDLC layers. Considering that the buffer layer with thickness t_n induces phase shift and has a refractive index nearly identical to the holographic diffraction structure, the transition matrix $\mathbf{A}^{n,m}$ can be represented as [16]:

$$\mathbf{A}^{n,m} = \exp\left[-i(\mathbf{k}_1^{n,m,n_h}\mathbf{y}_0)t_n\right]\begin{bmatrix}1 & 0\\ 0 & \exp\left[\frac{-i\Delta K^{n,m,n_h}t_n}{d_n}\right]\end{bmatrix} \quad (27)$$

These model components enable not only calculation of light intensity attenuation in the multilayer structure but also integration of structural inhomogeneity effects and those induced by external electric fields in each diffraction layer

$$\begin{cases} T_{01,10}^{n,m,n_h} = -i\frac{b_j^{n.m.n_h}}{2}\int\limits_{-1}^{1}\left(\frac{\exp\left(\frac{i\Delta K(1-q)}{1}\right)}{\cosh\left[\frac{cs(1+q)}{2}\right]^2}F_1 \right.\\ \quad \left.-\left(1-\frac{-b_j^{n,m,n_h}}{cs}, \frac{b_j^{n,m,n_h}}{cs}, 2, w(q)\right)dq\right)\\ T_{00,11}^{n,m,n_h} = 1-\frac{\left(b_j^{n.m.n_h}\right)^2}{2}A\int\limits_{-1}^{1}\left(\frac{\exp\left(\frac{i\Delta K(1-q)}{1}\right)}{\sinh\left[\frac{cs(1+q)}{2}\right]}{}_2F_1\right.\\ \quad \left.-\left(1-\frac{b_j^{n,m,n_h}}{cs}, 1+\frac{b_j^{n,m,n_h}}{cs}, 1, w(q)\right)dq\right), \end{cases} \quad (28)$$

where parameter ${}_2F_1$ — Gaussian hypergeometric function value, $\nu_j = \cos(\theta)_{rj}^{n,m,h}$,

$$w(q) = \frac{\sinh(cs(1-q)/2\sinh(cs(1+q)/2)}{\cosh(cs)\cosh(c(s-t))},$$

parameter θ_{rj}^{n,m,n_h} defines angles between group normals $\mathbf{N}_{rj}^{m,n,n_h}$ and the y axis corresponding to diffraction layer thickness,

$$b_p^{n,m,n_h}(E) = [d_n C_j^{n,m,n_h}(E)]/\sqrt{\nu_0\nu_1}$$

$$A = [cs\cosh(c\cdot t)\cosh(c(s-t))]^{-1}.$$

Within the proposed model, parameters c, s and $t$entering expression (28) quantitatively characterize three key aspects of spatial distribution: the degree of inhomogeneity (c), asymmetry level (s) and shift magnitude (t). For each individual layer of the multilayer structure, these parameters are determined by approximating the normalized spatial distribution $n_1(y)$ using the approximating function

$$n_1(y, c, s, t) = \mathrm{ch}^{-1}[c(sy-t)].$$

The obtained analytical expressions for transfer functions (18) enable quantitative description of selective optical properties of multiplexed chirped MIHDS sensitive to variations in external conditions, including electric field strength, incidence angle, and frequency composition of readout radiation. It should be noted that changes in external electric field strength on the structure alter the phase mismatch vector amplitude, as shown in [27]:

$$\Delta K^{n,m,n_k} = \Delta K^{n,m,n_h}(\theta) + \Delta K^{n,m,n_h}(\omega) + \Delta K^{n,m,n_h}(E), \quad (29)$$

where modules $\Delta K^{n,m,n_h}(\theta)$ and $\Delta K^{n,m,n_h}(\omega)$ quantitatively characterize the degree of phase synchronism violation arising from variations in angular and spectral characteristics of readout radiation.

Deviation from phase synchronism conditions under electric field strength influence can be determined as:

$$\Delta K^{n,m,n_h}(E) = \omega_{c_c}\left[n_0^{n,m,n_h}(E)(\mathbf{N}_0^{n,m,n_h}\mathbf{y}_0) - n_1^{n,m,n_h}(E)\,(\mathbf{N}_1^{n,m,n_h}\cdot\mathbf{y}_0)\right] + (\mathbf{K}^{n,m,n_h}\mathbf{y}_0).$$

The diffraction efficiency of multiplexed chirped MIHDS is defined as the ratio of energy flux density in the diffracted beam to the energy flux density in the incident radiation propagating along the normal to the interface. Considering that each monochromatic plane wave with complex amplitude $\mathbf{E}_j^{N,m,n_h}$ corresponds to a specific Poynting vector $\mathbf{S}_j^{N,m,n_h}$ integration over all frequency-angular spectra yields the integral expression for calculating total diffraction efficiency:

$$\eta_d^{N,m,n_h} = (S_1^{N,m,n_h}\mathbf{y}_0)/(\mathbf{S}_0^{N,m,n_h}\mathbf{y}_0), \quad (30)$$

where $\mathbf{y}_0$ — unit vector along the sample thickness,

$$\mathbf{S}_1^{N,m,n_h} = \mathbf{N}_1^{N,m,n_h}\frac{c^2}{(2\pi)^2}\iint(\mathbf{E}_1^{N,m}\mathbf{E}_1^{N,m,*})d\omega d\theta,$$

$$\mathbf{S}_0^{N,m,n_h} = \mathbf{N}_0^{N,m,n_h}\frac{c^2}{(2\pi)^2}\iint(\mathbf{E}_0^{N,m}\mathbf{E}_0^{N,m,*})d\omega d\theta.$$

Within subsequent numerical modeling, the interaction of plane quasi-monochromatic waves with unit amplitude and spatially inhomogeneous multiplexed chirped MIHDS containing composite photopolymer matrices with liquid crystals is considered. The input optical field amplitude is defined as $\mathbf{E}^0 = \delta(\omega, \theta)$, and its intensity as

$$\iint(\mathbf{E}^0\mathbf{E}^{0*})d\omega d\theta = 1.$$

With these notations, expression (20) can be transformed as:

$$\boldsymbol{\eta}_d^{N,m,n_h} = \frac{\mathbf{E}_1^{N,m}\mathbf{E}_1^{Nmm*}}{1} = \frac{|\mathbf{E}_1^{N,m}|^2}{1} = |E_1^{N,m,n_h}\omega\theta|^2, \quad (31)$$

where $E_1^{N,n_h}(\omega, \theta)$ is an element of the output optical field matrix $\mathbf{E}^{N,m}$ obtained by multiplying the transition matrices of all layers of the multiplexed chirped MIHDS.

Numerical Modeling

This subsection presents results obtained from numerical modeling based on the developed analytical models of light

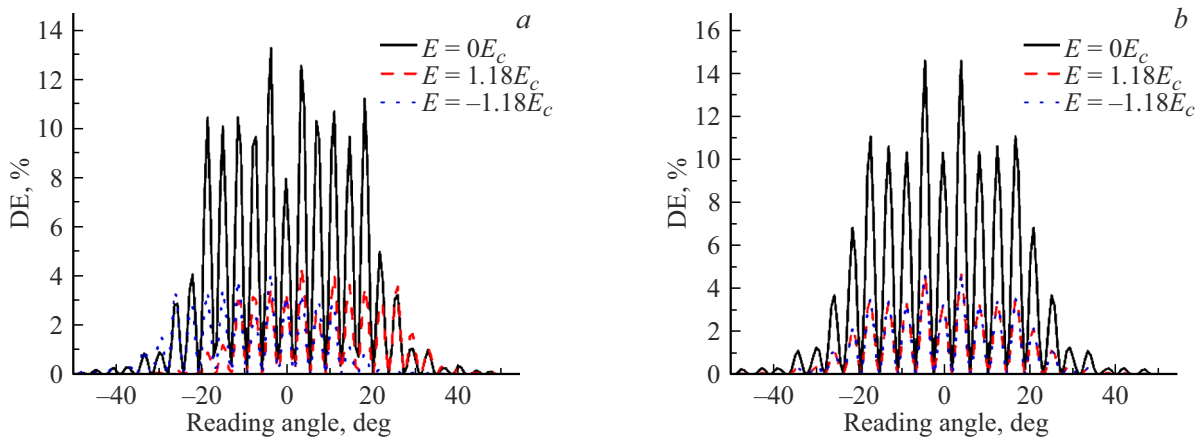

Figure 3. Dependence of selective response of chirped multiplexed MIHDS formed (*a*) in PPM-LC and (*b*) in PDLC with applied voltage across all diffraction layers.

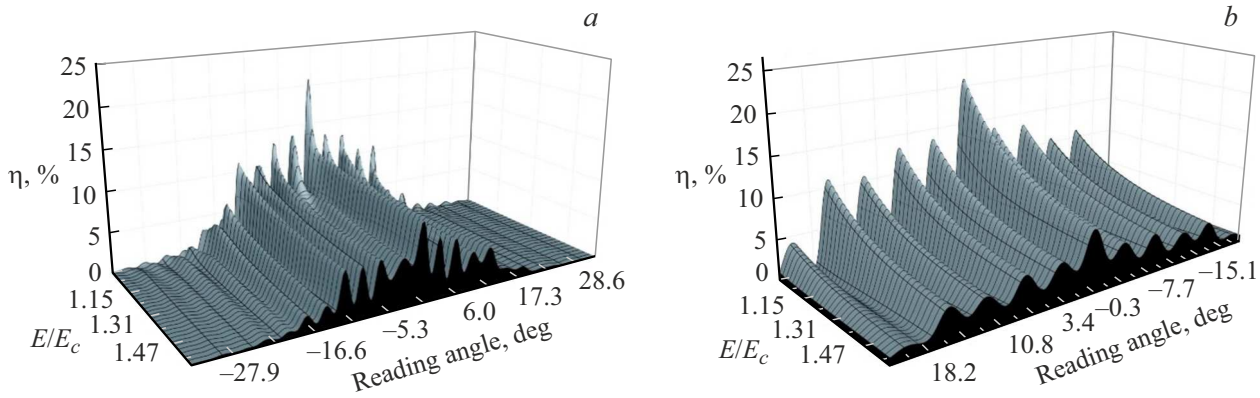

Figure 4. Dependence of selective response of chirped multiplexed MIHDS formed (*a*) in PPM-LC and (*b*) in PDLC with applied voltage to the second diffraction layer.

diffraction on MIHDS. Investigations focused on diffraction characteristics of multiplexed MIHDS formed from PPM-LC and PDLC.

Numerical modeling examined two-layer ($N = 2$) and three-layer ($N = 3$) HDS with uniform refractive index profiles, in which two chirped diffraction structures $\Psi_1 = -11^\circ$ and $\Psi_2 = 11^\circ$ were sequentially recorded at angles ($N_h = 2$) at wavelength $\lambda = 633$ nm with angles between recording beams of $2\theta = 20$. The thicknesses of the diffraction and buffer layers are $d_n = 20\,\mu$m and $t_n 120\,\mu$m respectively. $\Delta\theta = \theta_{\text{fal}} - \theta_{\text{B}}$ — readout angle relative to Bragg diffraction conditions.

From Fig. 3, *a*, it follows that when applying electric field strength above the critical Frederiks threshold with different polarities to all layers, a shift in selective response occurs: to the right for positive polarity and to the left for negative polarity, followed by DE reduction. For the structure shown in Fig. 3, *b*, the applied voltage polarity does not cause angular selectivity shift unlike the structure in Fig. 3, *a*, though DE reduction still occurs.

Figure 4 demonstrates that applying voltage to the second diffraction layer of a two-layer structure suppresses diffraction, consequently transforming the selective response to that of a single-layer structure, while retaining pronounced maxima characteristic of two-layer structures without zero-valued minima. This holds true for structures formed both in PPM-LC and PDLC.

Conclusion

This work presents for the first time generalized analytical models describing light diffraction on multiplexed chirped MIHDS for arbitrary light beam propagation, formed in photopolymer material with nematic liquid crystals as well as in polymer-encapsulated liquid crystals.

The effect of applied voltage on layers of multiplexed chirped MIHDS formed both in PPM-LC and PDLC has been demonstrated. It was shown that applying voltage of different polarities to all layers of PPM-LC structures results in selective response shifts in opposite directions. This fact demonstrates the potential for creating a spectral filter controllable both in level and wavelength, with each local maximum representing a separate channel.

It should also be noted that the chirping method enables broadening only the local maxima themselves, while multiplexing increases only their number. However, applying both methods simultaneously allows both broadening of angular selectivity for individual local maxima and increasing their quantity.

Conflict of interest

The authors declare that they have no conflict of interest.

References

[1] N. Vorzobova, P. Sokolov. Polymers, **11** (12), 1–14 (2020).
[2] A.O. Semkin, S.N. Sharangovich. Physics Procedia., **86**, 187–193 (2017). DOI: 10.1016/j.phpro.2017.01.020
[3] O.V. Sakhno, L.M. Goldenberg, J. Stumpe, T.N. Smirnova. J. Optics A: Pure and Appl. Optics, **11** (2), 024013 (2009). DOI: 10.1117/12.846463
[4] R. Hagen et al. Proc. SPIE, Digital Optical Technologies, **10335**, 103350D (2017). DOI: 10.1117/12.2270158
[5] G.B. Hadjichristov, Y.G. Marinov, G. Petrov. Proc. 10th Europ. Conference on Liquid Crystals ECLC, **525** (1), 128–139 (2010). DOI: 10.1080/15421401003796199
[6] S. Meng et al. Macromolecules, **40** (9), 3190–3197 (2007). DOI: 10.1021/ma070135q
[7] G. Zharkova et al. Microelectronic Engineering, **81** (2–4), 281–287 (2005). DOI: 10.1016/j.mee.2005.03.020
[8] S.V. Ustyuzhanin et al. TUSUR Reports, **2**, 192–197 (2007).
[9] A.O. Semkin, S.N. Sharangovich. Polymers, **11** (861), 1–14 (2019). DOI: 10.3390/polym11050861
[10] S.N. Sharangovich, V.O. Dolgirev, D.S. Rastrygin. Opt. i spektr., **133** (4), 359–368 (2025) (in Russian). DOI: 10.61011/OS.2025.04.60532.7513-24
[11] E.A. Dovol'nov, S.N. Sharangovich. Opt. i spektr., bf 105 (2), 336–345 (2008). (in Russian)
[12] A.S. Zadorin, S.N. Sharangovich. Opt. i spektr., bf 61 (3),–645 (1986). (in Russian)
[13] A.S. Zadorin, S.N. Sharangovich. Opt. i spektr., **59**(3), 592–596 (1985). (in Russian)
[14] S.N. Sharangovich. Opt. i spektr., **59** (4), 835–840 (1985). (in Russian)
[15] A.O. Semkin, S.N. Sharangovich. Bull. Russ. Acad. Sci. Phys., **77**, 1416–1419 (2013). DOI: 10.3103/S1062873813120125
[16] E.F. Pen, M.Y. Rodionov. Quant. Electron., **40**, 919–924 (2010). DOI: 10.1070/QE2010v040n10ABEH0 14360
[17] A. Yan, A. Liu, Y. Zhi, D. Liu, J. Sun. J. Opt. Soc. A., **26** (1), 135–141 (2009). DOI: 10.1364/JOSAA.26.000135
[18] G.P. Nordin, A.R. Tanguay. Opt. Lett., **17** (23), 1709–1711 (1992). DOI: 10.1364/JOSAA.9.002206
[19] V.O. Dolgirev, S.N. Sharangovich. Bull. Russ. Acad. Sci. Phys., **86** (1), 18–23 (2022). DOI: 10.3103/S106287382201021X
[20] N.A. Ivliev. Opt. Spectrosc., **129** (4), 400–405 (2021). DOI: 10.1134/S0030400X21040111
[21] A.O. Semkin, S.N. Sharangovich. Physics Procedia, **70**, 791–794 (2015). DOI: 10.1016/j.phpro.2015.08.269
[22] V.O. Dolgirev, S.N. Sharangovich, D.S. Rastrygin. Bull. Russ. Acad. Sci.: Phys., **88** (1), 6 (2024). DOI: 10.1134/S1062873823704865
[23] E.A. Dovolnov, S.N. Sharangovich, J.T. Sheridan. Trends in Optics and Photonics Series, 337 (2005). DOI: 10.1364/PEMD.2005.337
[24] B.F. Nozdrevatyh. Doklady TUSUR, **2** (16), 192–197 (2007). (in Russian)
[25] V.V. Shelkovnikov. Opt. i spektr., **97** (6), 1034–1042 (2004). (in Russian)
[26] S.N. Sharangovich. Radiotekhnika i elektronika, **40** (5), 1211–1222 (1995).
[27] O.A. Afonin. Pis'ma v ZhTF, **24** (11), 87–94 (1998). (in Russian)
[28] S.V. Ustyuzhanin. Phys. Wave Phenomena, **18**, 289–293 (2010). DOI: 10.3103/S1541308X10040102
[29] A.O. Semkin. Uchenye zapiski fizicheskogo fakul'teta MGU, **5**, 165306–1-165306–4 (2016). (in Russian)

Translated by J.Savelyeva